Journal of Advanced Marine Engineering and Technology, Vol. 50, No. 4, pp. 338~345, 2026
J. Advanced Marine Engineering and Technology (JAMET)
https://doi.org/10.5916/jamet.2026.50.4.338

ISSN 2234-7925 (Print)
ISSN 2765-4796 (Online)
Original Paper

Electromagnetic analysis of an axial-flux permanent magnet motor for torque density enhancement in electric propulsion systems

Wooyoung Choi[1] • Minsoo Park[2] • Byunghun Son[3] • Wooseok Han[4] • Bokyeong Chu[5] • Young Jin Hwang[†]

(Received May 4, 2026 ; Revised June 1, 2026 ; Accepted August 6, 2026)

Abstract: Axial-flux permanent magnet (AFPM) motors have gained significant attention in industries such as electric vehicles and marine applications due to their compact size, high torque density, and superior efficiency. While various AFPM designs have been proposed, this study focuses on the yokeless and segmented armature (YASA) topology, which offers unique advantages by eliminating the stator yoke. This reduces motor weight, thereby enhancing torque density, and decreases iron losses to improve overall efficiency. In this study, to further improve the overall performance of the YASA motor, a Halbach array was employed and an overhang structure also was introduced. To validate this approach, a comparative analysis was conducted using three-dimensional finite element method (3D FEM). The results demonstrate that incorporating the overhang structure in a YASA motor with Halbach array can significantly enhance its overall performance. This study shows the potential of AFPM motors not only in compact electric vehicles but also as a scalable solution for high-efficiency propulsion systems.

Keywords: Axial-flux permanent magnet (AFPM) motor, finite element analysis (FEA), Halbach array, overhang, Yokeless and segmented armature (YASA)

1. Introduction

Due to the increasing severity of environmental pollution and the strengthening of international carbon emission regulations, the demand for eco-friendly technologies has rapidly grown. Consequently, marine industry is accelerating their transition from conventional fossil-fuel-based propulsion systems to electric propulsion systems. Propulsion motors used in electric propulsion systems are required to simultaneously achieve high power density, high efficiency, and lightweight design, while accommodating limited installation space and diverse operating conditions. As a promising solution to meet these requirements, axial-flux permanent magnet (AFPM) motors have garnered considerable attention. Compared to radial-flux permanent magnet (RFPM) motors of the same volume, AFPM motors offer several advantages, including higher torque density, superior efficiency, and a more compact structure **[1]-[3]**. Due to these characteristics, AFPM motors have been actively studied in both academia and industry for various electrified applications, such as electric vehicles, marine propulsion systems, and aircraft **[4]-[7]**. Among the various AFPM motor topologies, the yokeless and segmented armature (YASA) type AFPM motor eliminates the stator yoke, thereby shortening the magnetic flux path and reducing unnecessary core volume. Consequently, YASA-type AFPM motors have been reported to exhibit superior efficiency, torque density, and power density compared with conventional AFPM topologies **[6],[8]**. Therefore, previous studies on AFPM motors have mainly focused on design optimization, enhancing motor performance, reducing torque ripple and cogging torque, and improving overall system efficiency **[9]-[17]**. These studies demonstrate that a Halbach array improves torque density due to its self-shielding effect **[12]-[13]**. In addition, to improve motor performance, an overhang structure can be applied to the rotor. The overhang structure allows the rotor magnets to be extended beyond the stator, effectively expanding the magnetic flux path and

† Corresponding Author (ORCID: http://orcid.org/0000-0003-1721-5596): Professor, Division of Electronics and Electrical Information Engineering, Korea Maritime & Ocean University, 727, Taejong-ro, Yeongdo-gu, Busan 49112, Korea, E-mail: yjhwang@kmou.ac.kr, Tel: 051-410-4411
1 M. S. Candidate, Major of Electrical and Electronic Engineering, Korea Maritime & Ocean University, E-mail: cyy2712@g.kmou.ac.kr
2 M. S. Candidate, Major of Electrical and Electronic Engineering, Korea Maritime & Ocean University, E-mail: ps6427@g.kmou.ac.kr
3 Research Engineer, Hyoseong Electric Company Ltd., E-mail: bhson@hyoseong.co.kr
4 Associate Research Engineer, Hyoseong Electric Company Ltd., E-mail: Wooseok.han@hyoseong.co.kr
5 Assistant Research Engineer, Hyoseong Electric Company Ltd., E-mail: chubk0710@hyoseong.co.kr

enabling greater flux concentration in the armature winding **[18]-[22]**. The overhang effect has been exploited in both axial and radial flux motors to enhance flux linkage and to improve output power. In the case of AFPM motors, the effect of the overhang structure can be obtained through a structure in which the radial length of the rotor is longer than the radial length of the stator. However, these studies have been independently conducted. As a result, there are few studies where these techniques have been applied together to analyze the overall performance of an AFPM motor.

In this paper, a comprehensive study is conducted to enhance the performance of a YASA-type AFPM motor. Specifically, the effect of the permanent magnet arrangement on the electromagnetic performance of the YASA motor is investigated by comparing a conventional permanent magnet configuration with a Halbach array. Additionally, to assess the influence of the overhang structure on motor performance, the overhang is applied to the rotor, and performance variations with and without the overhang were analyzed. Three-dimensional finite element analysis (3D FEA) is employed to comprehensively compare and evaluate the electromagnetic characteristics of each model. This study is expected to provide valuable design guidelines for improving the performance of YASA-type AFPM motors and to contribute to the development of electric propulsion motors that require high power density and high efficiency.

2. YASA Motor Design

An axial-flux permanent magnet (AFPM) motor with 12 stator slots and 10 poles, featuring a yokeless and segmented armature (YASA) with concentrated armature winding is considered. This study focused on a YASA motor with fundamental specifications, including an output power of 10 kW, a torque of 46.5 Nm, and a rated rotational speed of 2,100 r/min. The machine's specific dimensions were optimized through a multi-objective optimization approach. Simcenter Magnet Design Optimization 2021.1 software was used in this process. To validate the proposed 3D FEM model, the YASA-type AFPM motor reported in **[23]** was analyzed under the same specifications, and the simulation results were compared with the published experimental data. As shown in **Table 1**, the simulated rated power, rated torque, efficiency, and back-EMF agreed well with the experimental results, with a maximum error of 7.1%. The difference in efficiency is mainly attributed to mechanical losses, inverter losses, and manufacturing tolerances that were not fully considered in the simulation.

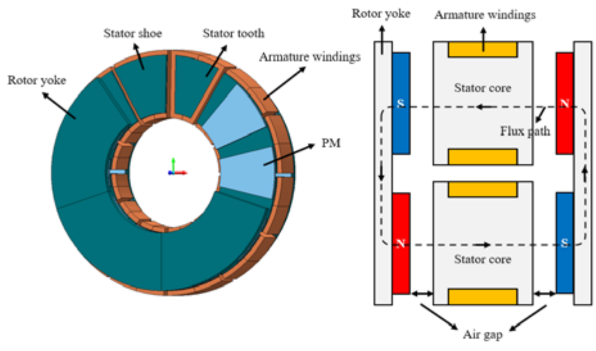

(a) (b)

Figure 1: Schematic configuration of the YASA motor: (a) whole structure, (b) cross-sectional structure

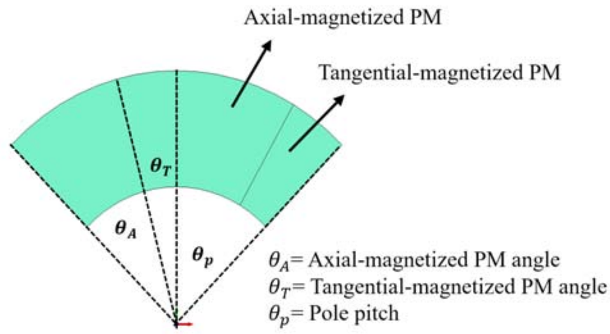

Figure 2: Definition of Halbach array

Table 1: Comparison of the Experimental and Simulated Results for the Reference YASA AFPM Motor.

Item	Ref. **[23]**	Simulation Result	Error Rate [%]
Topology	YASA	YASA	-
Slot/pole	12/10	12/10	-
Outer diameter [mm]	190	190	-
Rated power [kW]	6.28	6.31	0.48
Rated speed [r/min]	1,200	1,200	-
Rated torque [Nm]	50	50.2	0.4
Back-EMF [V]	70	70.44	0.63
Total efficiency [%]	90	96.4	7.1

Based on this validation, the proposed 3D FEM model was employed for the design and analysis of the proposed 10-kW AFPM motor.

Figure 1 illustrates the whole structure of a YASA motor. The motor consists of a dual rotor yoke, permanent magnets (PMs), and a stator with armature windings. The PMs are located on the surface of the rotor yoke and are made using N42-grade neodymium-iron-boron (NdFeB), a rare-earth material. In addition, 20PNF1500 electrical steel was used for both the rotor yoke and stator cores.

The Halbach array consists of axial-magnetized PMs that generate the main flux and tangential-magnetized PMs that assist the main flux by concentrating the magnetic field toward one side. In the proposed design, the magnet pole-arc ratio of the Halbach array can be defined as the ratio of the axial-magnetized PMs angle to the pole pitch, as shown in **Figure 2**.

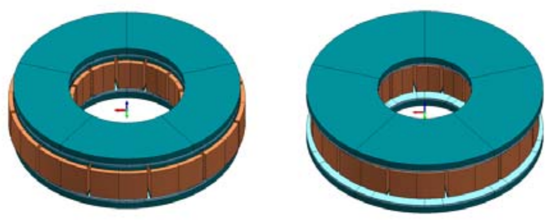

(a) (b)

Figure 3: 3D FEM model: (a) non overhang model, (b) overhang model.

Table 2: Design Specifications of the YASA Motor

Item	Unit	Value
Output power	kW	10
Phases	-	3
Rated frequency	Hz	175
Rated rotational speed	r/min	2,100
Air-gap length	mm	1.3
Outer diameter	mm	252
Inner diameter	mm	128.4
Motor axial length	mm	75.6
Number of slots	-	12
Number of poles	-	10
Filling factor	%	44.5
Current density	A/mm^2	8
Pole-arc ratio	-	0.7
PM thickness	mm	3.5

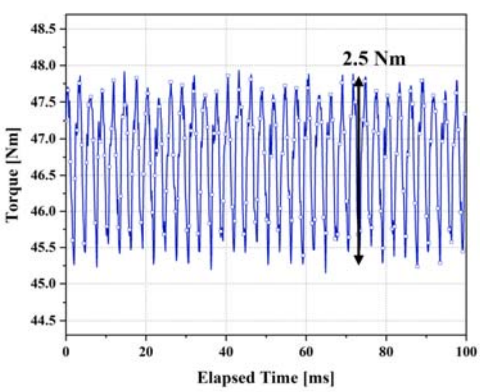

Figure 4: Simulation result of torque waveform and torque ripple of YASA motor; average torque = 46.5 Nm.

Figure 3 (a) and **(b)** present 3D finite element method (FEM) modeling images with and without the overhang structure of the YASA motor. In this study, we considered overhang lengths from 2 mm to 16 mm at 2 mm intervals. An overhang structure was applied to the rotor to account for the influence of the stator end-winding region, and its effect on electromagnetic performance was analyzed. **Table 2** and **Figure 4** show the initial design specifications and output torque waveform of the YASA motor.

3. Simulation Results and Discussion

The conventional YASA motor produced an average torque of 46.5 Nm with a peak-to-peak torque ripple of approximately 2.5 Nm as shown in **Figure 4**. In this study, a Halbach array and an overhang structure were applied to enhance the performance of the YASA motor. The electromagnetic characteristics of each model were comparatively analyzed through electromagnetic simulations.

3.1 Halbach Array

The Halbach array is a special arrangement of PMs, characterized by amplifying the magnetic field on one side of the Halbach array and bringing the magnetic field on the other close to zero. This arrangement can improve motor performance. In this study, the performance of the Halbach array YASA motor was evaluated by varying the pole-arc ratio, while keeping all other design parameters constant.

Figure 5 presents the simulation results of average torque and torque per magnet volume under different pole-arc ratios for the YASA motor and the Halbach array YASA motor.

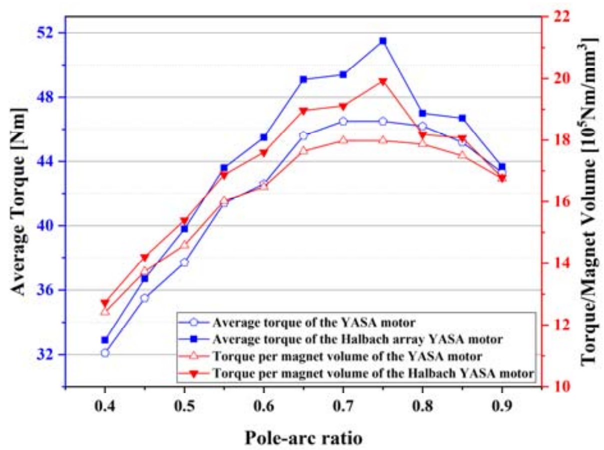

Figure 5: Comparison of average torque and torque per magnet volume under different pole-arc ratios for YASA motor and Halbach array YASA motor

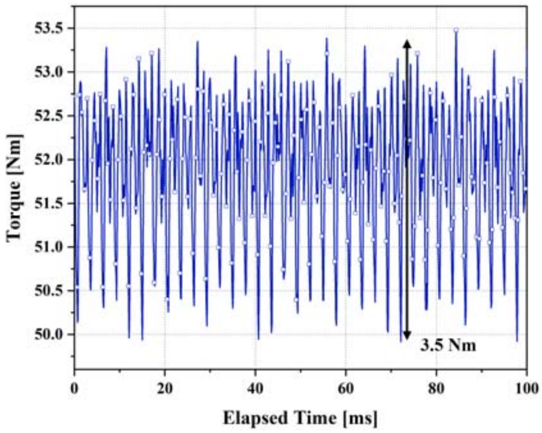

Figure 6: Simulation result of torque waveform and torque ripple of Halbach array YASA motor; average torque = 51.5 Nm.

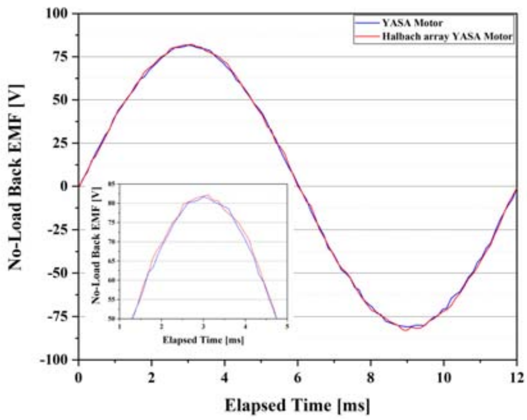

(a)

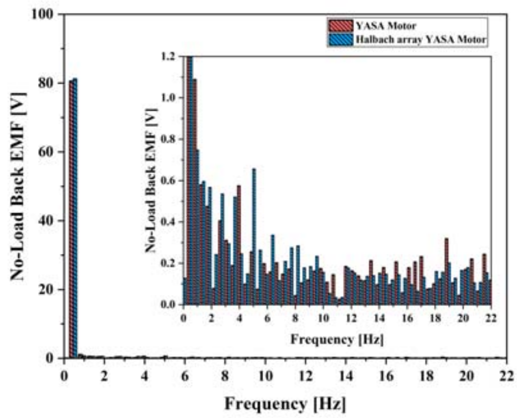

(b)

Figure 7: Comparison of no-load back-EMF waveforms and harmonic spectra of the YASA motor and Halbach array YASA motor. (a) no-load back-EMF waveform, (b) harmonic spectra

The results indicate that the torque initially increases and then decreases as the pole-arc ratio increases, with a maximum torque of 51.5 Nm at a pole-arc ratio of 0.75. When the pole-arc ratio of the YASA motor is 0.7, the output torque is 46.5 Nm. The output torque of the Halbach array YASA motor is 9.71% higher than that of the conventional YASA motor. In addition, its torque per magnet volume is increased by 9.4% compared with that of the traditional one. This indicates that the Halbach array configuration improves permanent magnet utilization by generating higher torque output for a given magnet volume.

Figure 6 shows simulation results of the torque waveform and torque ripple of Halbach array YASA motor at a pole-arc ratio of 0.75. The torque ripple of the Halbach array YASA motor was 3.5 Nm (peak-to-peak), corresponding to 6.7% of the average torque.

In addition, a no-load analysis is conducted to evaluate the total harmonic distortion (THD) of the back electromotive force (Back-EMF). A higher THD in the back-EMF can cause torque ripple and additional losses during motor operation and consequently a lower THD is required. The THD of the no-load back EMF is calculated by using **Equation (1)**.

$$THD = \frac{\sqrt{V_2^2+V_3^2+V_4^2+\cdots}}{V_1} \times 100[\%] \tag{1}$$

Figure 7(a) and **(b)** presents the back-EMF waveforms and harmonic spectra of both models. The inset in **Figure 7(a)** provides a zoomed view of the positive back-EMF waveform. **Figure 7(b)** shows the harmonic components obtained from the fast fourier transform (FFT) analysis of the back-EMF waveform. The inset in **Figure 7(b)** shows a zoomed view of the harmonic spectrum for clearer comparison. While the THD of the traditional YASA motor was calculated to be 4.12 %, that of the Halbach array YASA motor was 3.8%, representing an approximately 7.7 % reduction.

3.2 Overhang Effect

Owing to improve motor performance, an overhang structure can be applied to the rotor. Both the conventional YASA model and the Halbach array YASA model were analyzed for cases without overhang and with overhang lengths from 2 to 16 mm, in 2 mm increments. An increase in overhang length can enhance machine performance by improving magnetic flux utilization. However, if the overhang length becomes excessive, magnetic saturation may occur in the stator core, resulting in a decline in performance. Therefore, to achieve optimal machine performance, it is essential to select an appropriate overhang length while taking into account the magnetic saturation characteristics of the stator core. To investigate the effect of overhang, electromagnetic analyses were conducted on both the conventional YASA motor and the Halbach array YASA motor, using identical design specifications and rotational speeds. The only variable altered during the analysis was the overhang length.

Figure 8 and **Figure 9** show the electromagnetic performance and loss characteristics of the YASA motor according to the overhnag length. The analysis results indicate that both torque and output power generally exhibited an upward trend as the overhang length increased. Although ohmic and iron losses increased with longer overhang lengths, the efficiency of the 8 mm overhang model was calculated to be 97.7%, comparable to that of the non-overhang model when accounting for electrical losses. This indicates that the 8 mm overhang model can improve output power by approximately 17.1% compared to the conventional YASA motor while maintaining a similar efficiency level. In contrast, the efficiency of the 16 mm overhang model dropped to 96.4%, likely due to increased losses and magnetic saturation in the stator core caused by excessive overhang length.

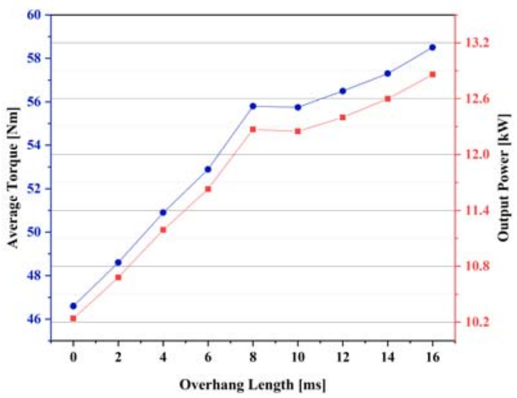

Figure 8: Average torque and output power of YASA motor according to overhang length

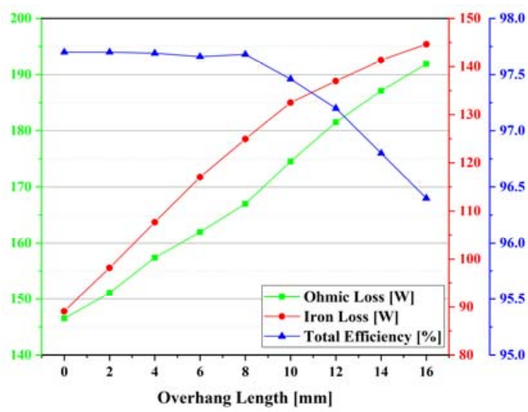

Figure 9: Ohmic loss, iron loss, and total efficiency of YASA motor according to overhang length

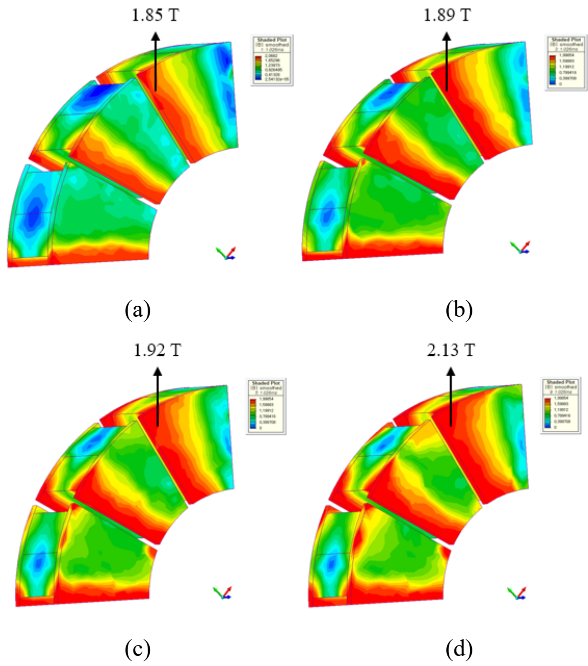

Figure 10: Magnetic field distribution of YASA motor: (a) non overhang model (1.85T), (b) 4 mm overhang model (1.89 T), (c) 8 mm overhang model (1.92 T), and (d) 16 mm overhang model (2.13 T)

Figure 10 presents the magnetic flux density distribution of the YASA motor for different overhang lengths. As the overhang length increases, more magnetic flux links with the stator winding, thereby enhancing torque and output power. In the 8 mm overhang model, the maximum flux density was 1.92 T, indicating that the stator core remained within an acceptable magnetic saturation range. In contrast, the 16 mm overhang model exhibited a maximum flux density of 2.13 T, confirming the occurrence of magnetic saturation in the stator core. Therefore, considering output performance, efficiency, and magnetic saturation characteristics, the 8 mm overhang length was selected as the design value.

As shown in **Figure 11**, **Figure 12**, and **Figure 13**, the Halbach array YASA motor exhibited electromagnetic performance and loss characteristics similar to those of the conventional YASA motor concerning the overhang length. As the overhang length increased, torque and output power generally improved due to enhanced magnetic flux utilization. However, under conditions of excessive overhang length, performance gains were limited by increased losses and magnetic saturation in the stator core. The Halbach array YASA motor with a 12 mm overhang demonstrated the highest torque and output power, achieving an approximately 15.9% improvement compared to the non-overhang model. The optimal overhang length of the Halbach array YASA motor was larger than that of the conventional YASA motor.

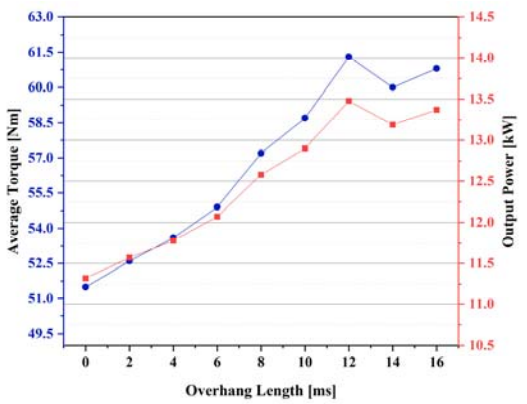

Figure 11: Average torque and output power of Halbach array YASA motor according to overhang length.

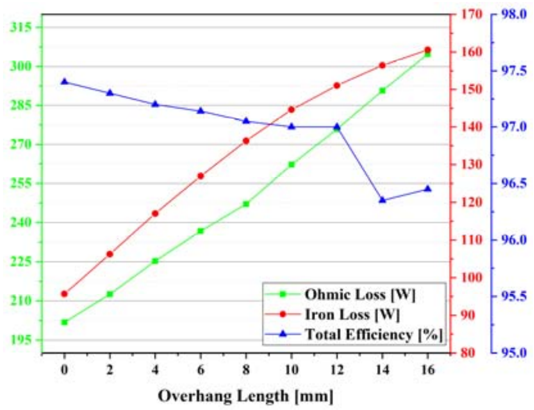

Figure 12: Ohmic loss, iron loss, and total efficiency of Halbach array YASA motor according to overhang length.

This is because the Halbach array YASA motor concentrates magnetic flux toward the air gap, enabling the additional magnetic flux in the overhang region to contribute more effectively to torque generation. Consequently, the torque and output power increase over a longer overhang range compared to the conventional YASA motor, leading to a larger optimal overhang length of 12 mm. This result indicates that combining the Halbach array with an overhang structure can further enhance electromagnetic performance compared to using the Halbach array alone. Under these conditions, the maximum flux density was 1.97 T, indicating that the stator core remained within an acceptable magnetic saturation range. In contrast, when the overhang length exceeded 12 mm, the maximum flux density reached 2.2 T, indicating magnetic saturation in the stator core, as shown in **Figure 13**.

Table 2 summarizes the overall electromagnetic performance of the analyzed models. The reported efficiency was calculated under the assumption that only electrical losses, such as iron loss and ohmic loss, were considered. These results demonstrate that

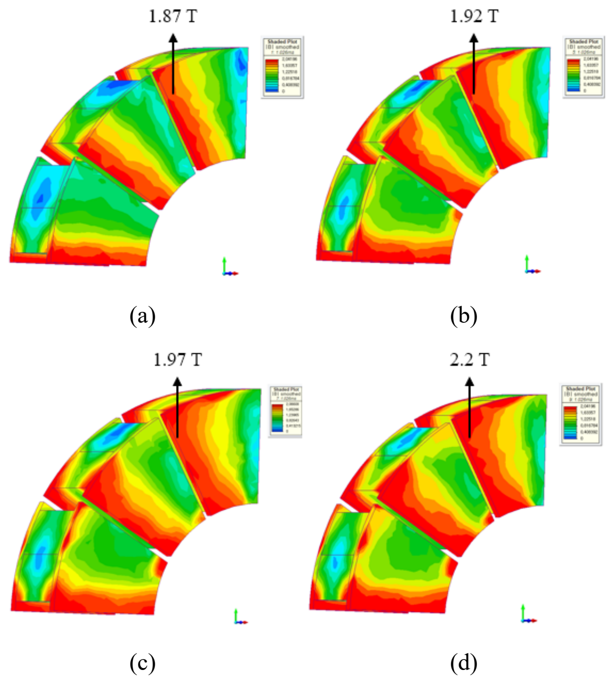

Figure 13: Magnetic field distribution of Halbach array YASA motor: (a) non overhang model (1.87 T), (b) 8 mm overhang model (1.92 T), (c) 12 mm overhang model (1.97 T), and (d) 16 mm overhang model (2.2 T)

Table 2: Comparison of Electromagnetic Performance

Item	YASA		Halbach array YASA	
Overhang length [mm]	0	8	0	12
Output power [kW]	10.2	12.3	11.3	13.5
Torque [Nm]	46.5	55.8	51.5	61.3
Efficiency [%]	97.7	97.7	97.4	97
Torque density [Nm/dm^3]	16.65	19.92	18.45	21.51
THD [%]	4.12	4.19	3.8	4.02

applying a Halbach array and an overhang structure to a YASA motor can significantly enhance its overall electromagnetic performance. In particular, the YASA motor employing both the Halbach array and the overhang structure exhibited an approximately 22.5% improvement in torque density compared to the conventional YASA motor.

4. Conclusion

In this study, the effects of Halbach array and overhang on a YASA motor were analyzed based on 3D FEM. The Halbach array was applied to the conventional YASA motor to enhance magnetic flux concentration and PM utilization. Simulation results demonstrated that the Halbach array YASA motor achieved a 9.71% increase in output torque and a 9.4% improvement in torque per magnet volume compared to the conventional YASA motor. The overhang effect was then analyzed by varying the overhang length. For the conventional YASA motor, the 8 mm overhang model was selected as the appropriate design considering output power, efficiency, and magnetic saturation characteristics. Furthermore, the combined application of the Halbach array and the overhang structure resulted in the most significant performance improvement. The Halbach array YASA motor with a 12 mm overhang achieved the highest torque and output power, demonstrating an approximate 15.9% increase compared to the non-overhang Halbach array model. Additionally, the torque density improved by approximately 22.5% compared to the conventional YASA motor, further verifying the effectiveness of the proposed design in enhancing the electromagnetic performance of the YASA motor. These results can be considered an effective approach for improving the torque density and electromagnetic performance of YASA-type AFPM motors for electric propulsion systems.

Acknowledgement

This paper was supported by Korea Institute for Advancement of Technology (KIAT) grant funded by the Korea Government (MOTIE) (RS-2024-00424595 / Regional Residency Program for Cultivating Advanced Research Talent in Next-Generation Marine Mobility Industry Innovation), and the National Research Foundation of Korea (NRF) grant funded by the Korea government (MSIT) (No. RS-2024-00391886). (Corresponding author: Young Jin Hwang.)

Author Contributions

Conceptualization, W.-Y. Choi; Methodology, W.-Y. Choi; Software, W.-Y. Choi; Validation, W.-Y. Choi, M.-S. Park, B.-H. Son, W.-S. Han, B.-G. Chu; Formal Analysis, W.-Y. Choi; Investigation, W.-Y. Choi; Resources, W.-Y. Choi; Data Curation, W.-Y. Choi; Writing—Original Draft Preparation, W.-Y. Choi; Writing—Review & Editing, Y.-J. Hwang; Visualization, W.-Y. Choi; Supervision, Y.-J. Hwang; Project Administration, Y.-J. Hwang; Funding Acquisition, Y.-J. Hwang.

References

[1] L. Shao, R. Navaratne, M. Popescu, and G. Liu, “Design and construction of axial-flux permanent magnet motors for electric propulsion applications—A review,” IEEE Access, vol. 9, pp. 158998-159017, Nov. 2021.

[2] Z. Hao, Y. Ma, P. Wang, G. Luo, and Y. Chen, “A review of axial-flux permanent-magnet motors: topological structures, design, optimization and control techniques,” Machines, vol. 10, no. 12, p. 1178, Dec. 2022.

[3] S. Kahourzade, A. Mahmoudi, H. W. Ping, and M. N. Uddin, “A comprehensive review of axial-flux permanent magnet machines,” Canadian Journal of Electrical and Computer Engineering, vol. 37, no. 1, pp. 19-33, 2014.

[4] A. Havel, M. Sobek, L. Stepanec, and J. Strossa, “Optimization of permanent magnet parameters in axial flux rotary converter for HEV drive,” Energies, vol. 15, no. 3, p. 724, Jan. 2022.

[5] V. Di Dio, G. Cipriani, and D. Manno, “Axial flux permanent magnet synchronous generators for pico hydropower application: A parametrical study,” Energies, vol. 15, no. 19, p. 6869, Sep. 2022.

[6] J. Chang, Y. Fan, J. Wu, and B. Zhu, “A yokeless and segmented armature axial flux machine with novel cooling system for in-wheel traction applications,” IEEE Transactions on Industrial Electronics, vol. 68, no. 5, pp. 4131-4140, May. 2021.

[7] Z. Zhan, W. Geng, Y. Liu, and C. Wang, “Feasibility of a new ironless-stator axial flux permanent magnet machine for aircraft electric propulsion application,” CES Transactions on Electrical Machines and Systems, vol. 3, no. 1, pp. 30-38, Mar. 2019.

[8] T. J. Woolmer and M. D. McCulloch, “Analysis of the Yokeless and Segmented Armature Machine,” 2007 IEEE International Electric Machines & Drives Conference, pp. 704-708, May. 2007.

[9] L. Xu, Y. Xu, J. Xu, B. Wang, and F. Xin, “Optimal design and electromagnetic analysis of yokeless and segmented armature machine based on finite-element method and genetic algorithm,” 2017 IEEE Transportation Electrification Conference and Expo, pp. 1-6, 2017.

[10] Z. Zhang, C. Wang, and W. Geng, “Design and optimization of halbach-array PM rotor for high-speed axial-flux permanent magnet machine with ironless stator,” in IEEE Transactions on Industrial Electronics, vol. 67, no. 9, pp. 7269-7279, Sep. 2020.

[11] A. Habib, H. Che, N. Rahim, M. Tousizadeh, and E. Sulaiman, “A fully coreless Multi-Stator Multi Rotor

(MSMR) AFPM generator with combination of conventional and Halbach magnet arrays," Alexandria Engineering Journal, vol. 59, no. 2, pp. 589-600, 2020.

[12] Y. Lu, Y. Kai, S. Songjun, L. Yixiao, X. Fei, and L. Cheng, "Study on the influence of a combined-halbach array for the axial flux permanent magnet electrical machine with yokeless and segmented armature," in IEEE Transactions on Magnetics, vol. 60, no. 3, pp. 1-5, Mar. 2024.

[13] P. Srikhumphun, *et al.*, "Design optimization and comparative study of skewed halbach-array magnets TORUS axial-flux permanent magnet motors for electric vehicles," IEEE Access, vol. 12, pp. 99912-99920, 2024.

[14] M. Aydin, Z. Q. Zhu, T. A. Lipo, and D. Howe, "Minimization of cogging torque in axial-flux permanent-magnet machines: design concepts," IEEE Transactions on Magnetics, vol. 43, no. 9, pp. 3614-3622, Sep. 2007.

[15] C. -C. Hwang, P. -L. Li, F. C. Chuang, C. -T. Liu, and K. -H. Huang, "Optimization for reduction of torque ripple in an axial flux permanent magnet machine," IEEE Transactions on Magnetics, vol. 45, no. 3, pp. 1760-1763, Mar. 2009.

[16] F. Giulii, G. De Donato, and F. Caricchi, "Recent advances in axial-flux permanent-magnet machine technology," IEEE Transactions on Industry Applications, vol. 48, no. 6, pp. 2190-2205, Dec. 2012.

[17] H. S. Kwon, H. K. Yeo, and H. K. Jung, "Influence of a novel flux-absorbing structure on the performance of a surface-mounted permanent-magnet motor with overhang," IET Electric Power Applications, vol. 13, no. 12, pp. 2096-2102, Dec. 2019.

[18] H. J. Park, H. -K. Jung, S. -Y. Jung, Y. -H. Chae, and D. -K. Woo, "Field reconstruction method in axial flux permanent magnet motor with overhang structure," in IEEE Transactions on Magnetics, vol. 53, no. 6, pp. 1-4, Jun. 2017.

[19] H. K. Ye, D. -K. Lim, D. -K. Woo, J. Ro, and H. -K. Jung, "Magnetic equivalent circuit model considering overhang structure of a surface mounted permanent-magnet motor," IEEE Transactions on Magnetics, vol. 51, no. 3, pp. 1-4, Mar. 2015.

[20] M. M. Koo, J. -Y. Choi, Y. -S. Park, and S. -M. Jang, "Influence of rotor overhang variation on generating performance of axial flux permanent magnet machine based on 3-D analytical method," IEEE Transactions on Magnetics, vol. 50, no. 11, pp. 1-5, Nov. 2014.

[21] Y. D. Chun, J. Lee, and S. Wakao, "Overhang effect analysis of brushless DC motor by 3-D equivalent magnetic circuit network method," IEEE Transactions on Magnetics, vol. 39, no. 3, pp. 1610-1613, May. 2003.

[22] Y. J. Hwang, J. Y. Jang, and H. Jeon, "Overhang effect analysis of a homopolar HTS synchronous generator using 3D finite element method," IEEE Transactions on Applied Superconductivity, vol. 30, no. 4, pp. 1-5, Jun. 2020.

[23] W. Fei, P. C. K. Luk, and K. Jinupun, "A new axial flux permanent magnet segmented-armature-torus machine for in-wheel direct drive applications," 2008 IEEE Power Electronics Specialists Conference, pp. 2197–2202, Jun. 2008.